Pure and Applied Geophysics

Global Event Location with Full and Sparse Data Sets Using Three-dimensional Models of Mantle *P*-wave Velocity

Mchael Antolik,[1] Göran Ekström,[1] and Adam M. Dziewonski[1]

Abstract — In order to improve on the accuracy of event locations at teleseismic distances it is necessary to adequately correct for lateral variations in structure along the ray paths, either through deterministic model-based corrections, empirical path/station corrections, or a combination of both approaches. In this paper we investigate the ability of current three-dimensional models of mantle *P*-wave velocity to accurately locate teleseismic events. We test four recently published models; two are parameterized in terms of relatively long-wavelength spherical harmonic functions up to degree 12, and two are parameterized in terms of blocks of constant velocity which have a dimension of a few hundreds of km. These models, together with detailed crustal corrections, are used to locate a set of 112 global test events, consisting of both earthquakes and explosions with *P*-wave travel-time data compiled by the International Seismological Centre (ISC). The results indicate that the supposedly higher resolution block models do not improve the accuracy of teleseismic event locations over the longer wavelength spherical harmonic models. For some source locations the block models do not predict the range of observed travel-time residuals as well as the longer wavelength models. The accuracy of the locations largely varies randomly with geographic position although events in central Asia are particularly well located. We also tested the effect of reduced data sets on the locations. Multiple location iterations using 30 *P*-wave travel times indicate that teleseismic events may be located within an area of 1000 km² of the true location 66% of the time with only the model-based corrections, and increasing to 75% if calibration information is available. If as few as 8 phases are available then this is possible only 50% of the time. Further refinement in models and/or procedure, such as the addition of P_n phases, azimuth data, and consideration of *P*-wave anisotropy may provide further improvement in the teleseismic location of small events.

Key words: Event location, seismic tomography, mantle heterogeneity.

Introduction

One stated technical goal for monitoring of the Comprehensive Nuclear-Test-Ban Treaty (CTBT) is to locate events of $M \geq 4$ with an estimated uncertainty of 1000 km² or less for the purpose of on-site inspection. Because of the lateral heterogeneities present within the real earth, this goal is usually not achieved using conventional location techniques with standard one-dimensional velocity models. Two general approaches can be used to improve the quality of locations. The first is

---

[1] Department of Earth and Planetary Sciences, Harvard University, Hoffman Laboratory, Cambridge, MA 02138, U.S.A.

the application of empirically derived station corrections. While such corrections are only calculated once and then stored, and therefore can be applied extremely quickly in most location algorithms, they are often critically dependent on the source region. Station corrections which are regionally invariant often give little or no improvement in location. Further, the application of source-region dependent corrections depends upon previous sampling of ray paths from all possible source regions. The second approach is the use of a laterally varying earth model. While this approach does not suffer from the above disadvantage, it requires the calculation of a travel-time correction for each ray. In addition, the potential resolution of laterally heterogeneous models is limited by the quality and coverage of the data employed, and also by the computational resources available for their derivation.

Global three-dimensional (3-D) velocity models of the earth's mantle continue to evolve and become parameterized on an ever finer scale. Models of both compressional and shear-wave velocity are now commonly parameterized in terms of constant velocity blocks (e.g., VASCO and JOHNSON, 1998; GRAND *et al.*, 1997; VAN DER HILST *et al.*, 1997; BOSCHI and DZIEWONSKI, 1999a) rather than spherical harmonic functions. Such "high-resolution" models, using blocks with sizes on the order of a few hundred kilometers, have provided sharper images of coherent smaller-scale heterogeneities, in particular fast, sheet-like anomalies presumed to correspond to slabs penetrating the lower mantle. These models should lead to better characterization of *P*-wave residuals for paths through subduction zones or other areas where small-scale lateral heterogeneities are present. However, a number of factors may lead to lower resolution of large-scale, smaller amplitude anomalies in block models. Because of the higher number of unknown parameters, it is still impractical to invert combinations of very large data sets (waveforms and travel times), as is frequently done with spherical harmonic models (SU and DZIEWONSKI, 1997; LI and ROMANOWICZ, 1996). This may result in lower resolution in certain areas (particularly the shallow mantle) to which particular data sets are sensitive. In addition, the division into arbitrary, constant velocity blocks may induce an unrealistic shape in long-wavelength anomalies. A lack of correlation between new, high-resolution earth models and earlier longer wavelength models has previously been noted (GRAND *et al.*, 1997). Another possible factor in this discrepancy may be the use of regularization or damping in the solution of the inverse problem (BOSCHI and DZIEWONSKI, in press).

Recently, the work of SMITH and EKSTRÖM (1996) has shown that spherical harmonic models of *P*-wave velocity are of sufficient quality to be useful in improving teleseismic event locations. By inverting *P*-travel times from a data set of events with known or very accurately determined "ground-truth" locations, they demonstrated that the average mislocation distance was reduced by approximately 40% using the 3-D model S&P12/WM13 (hereafter referred to as SP12) (SU *et al.*, 1994) as compared to PREM or IASPEI91. However, only small improvements were obtained for earthquakes occurring in geologically complex areas along plate

boundaries, presumably due to the inadequate representation in SP12 of anomalies with wavelengths of a few hundred kilometers or less. On the other hand, this may be due to the fact that most of these latter events are earthquakes with less accurate ground-truth locations.

In this paper we use essentially the same data set as that used by SMITH and EKSTRÖM (1996) (hereafter SE96), with additional explosions from the Chinese Lop Nor test site. We test the improvement which can be obtained in teleseismic event location using the newer block models of mantle *P*-wave velocity compared to spherical harmonic models and to PREM. The performance of PREM compared to other global 1-D models such as IASPEI91 or the tables of JEFFREYS and BULLEN (1958) has already been tested by SE96. We concentrate only on models of *P*-wave velocity since block models of shear velocity are as yet few in number, and previous work using *S* waves has shown them to be mostly of use in improving depths rather than epicentral locations (EKSTRÖM *et al.*, 1997) due to the larger picking errors associated with them. We test the models both with and without empirical station corrections. After a brief description of the models and of the location method, the Analysis section of the paper discusses the accuracy of locations obtained using the entire ISC *P*-wave data set for each model and with different combinations of station corrections employed.

Since the terms of the CTBT require the elimination of nuclear tests of all yields, it is also desirable to examine the utility of 3-D models for the location of small or moderate sized events (*M* 4–5). At teleseismic distances, small magnitude events may be recorded by only a few stations. We have therefore conducted experiments in which only a portion of the available *P*-wave data is used and examined the performance of each of the 3-D models relative to PREM. These results are presented in the second half of the Analysis section. Using data sets consisting of 30 phases, the 3-D models are able to locate the test events to within the accuracy goal of the CTBT on the order of 70% of the time. The results improve when using station corrections derived from the ground-truth locations of nearby test events.

3-D Models and Event Data

We test four 3-D models in this paper. In assessing the accuracy in event location obtained by the various models, it is important to keep in mind the data used in constructing each model as well as the inversion method. Model SP12 was obtained by SU and DZIEWONSKI (1993) through joint inversion of both *P*- and *S*-wave travel times compiled by the ISC and differential travel times compiled by other researchers. To improve resolution in the mid-mantle, they also employed long-period body and mantle waveform data. Their starting model was obtained by adapting and scaling an earlier shear-wave velocity model (SU *et al.*, 1994). The final

model is parameterized horizontally in terms of spherical harmonics up to degree 12 and radially in terms of Chebyshev polynomials up to order 13. This provides a nominal radial resolution on the order of 200 km and a horizontal resolution of about 1,700 km. Although this resolution is rather low, SE96 obtained an average reduction in mislocation distance of 40% over standard 1-D models using SP12 for explosions with known locations.

Su and Dziewonski (1997) subsequently carried out a joint inversion for shear and bulk sound velocity in the mantle using much of the same data. Approximately 40,000 waveforms and well over a million travel times were used. Their final models were obtained in two stages; first by solving for the perturbations in shear modulus only, and then by adding perturbations in the bulk modulus. They used the same parameterization as in SP12 and the same starting model. We test a *P*-velocity model derived from the bulk sound and shear velocity models (referred to as MK12).

The other two 3-D models that we test are parameterized in terms of blocks having a constant velocity. The first of these is Model BDP98, obtained by Boschi and Dziewonski (1999a) using ISC residuals from epicenters corrected for lateral heterogeneity using model SP12. The model describes *P*-wave velocity with respect to PREM. The blocks have a dimension of $5° \times 5°$ at the equator (roughly equivalent to spherical harmonic degree 40). The area of the blocks is kept constant from the equator to the poles. In their inversion, Boschi and Dziewonski heavily damped the roughness of the solution over its norm. The second block model is that obtained by van der Hilst *et al.* (1997), who used *P*-wave residuals derived from the new locations published in Engdahl *et al.* (1998). We refer to this model as HWE97. HWE97 describes *P*-velocity anomalies with respect to the 1-D model ak135 Kennett *et al.* (1995). Its parameterization is in $2° \times 2°$ blocks where the area of the blocks is not preserved. Boschi and Dziewonski (1999a) compare the spherical harmonic spectra of these two models, and note that BDP98 has higher power at lower degrees than HWE97 but a far more rapid decay in power at higher degrees.

The set of test events which we employ to test these models is the same as that used by SE96, with the addition of additional explosions at the Chinese Lop Nor test site for which accurate ground-truth information is available from satellite data (Wallace and Tinker, 2001). Figure 3 shows the locations of these events. There are 30 explosions and 82 earthquakes. The epicentral information for the explosions has been determined by non-seismic means, while the location accuracy for the earthquakes has been reported as 5 km and the origin time uncertainty as 0.5 s (Kennett and Engdahl, 1991). From these events we first use all of the *P* phases in the ISC catalog in the distance range $25°$ to $96°$. The number of available phases ranged from about 45 to over 500, and the events range in magnitude from m_b 5.0 to 7.5. Next we investigate the effect of using a sparse data set by restricting the number of phases to first 30 and then to 8.

Procedure

Following SE96, we compute separate travel-time perturbations for each *P*-wave raypath used in the inversions corresponding to the effects of mantle structure, crustal structure, ellipticity, and station elevation, which are then added to the travel time calculated for the reference model (PREM or ak135). For the spherical harmonic models, the mantle structure corrections are obtained using the method of DZIEWONSKI (1984) which uses coordinate rotations and an integral table to achieve rapid calculation of the travel-time perturbation corresponding to each coefficient of the spherical harmonic expansion. We take advantage of Fermat's principle in assuming that the mantle corrections are stationary with respect to small changes in the raypath [SE96] (i.e., the assumed raypath is that in the reference model). For block models the mantle correction is simply

$$\delta t_M = -\sum_{i=1}^{N} dt_i \left(\frac{\delta v}{v_o}\right)_i \tag{1}$$

where dt_i is the travel time in the *i*th block, and the expression in parentheses is the velocity perturbation of the *i*th block with respect to the reference 1-D velocity (v_o).

Crustal corrections are incorporated into the relocations in two ways. The first is a degree 12 spherical harmonic expansion of the ocean-contintent function and is described in SU *et al.* (1994). The expansion is normalized to give an average crustal thickness of 24.4 km. We also employed the full CRUST5.1 model of MOONEY *et al.* (1998), which is defined in $5° \times 5°$ blocks. This correction was applied by calculating travel time for a ray through this model having the same slowness as in the reference 1-D model. Both source and receiver-side corrections were used. Corrections for crustal structure can be quite large in regions of thick crust, and are negative in the ocean basins (Fig. 1). We calculated the elevation correction by assuming a vertical raypath through crust with an average velocity of 5.8 km s^{-1}.

Station Corrections

We investigated the use of empirical station corrections with the 3-D models in an attempt to correct for unmodeled structure. Despite the high resolution of the block models, we expect that shallow, localized anomalies with wavelengths less than $\sim$100 km may introduce significant error into locations determined from the mantle models alone, as may deeper, longer wavelength anomalies if their amplitudes are not as well determined as in lower resolution models. We calculated region-dependent corrections by dividing the earth into bins 5° wide in azimuth and either 2.5° or 5° wide in epicentral distance. No correction is made for event depth. We then use one of the 3-D models to relocate all of the events in the compilation
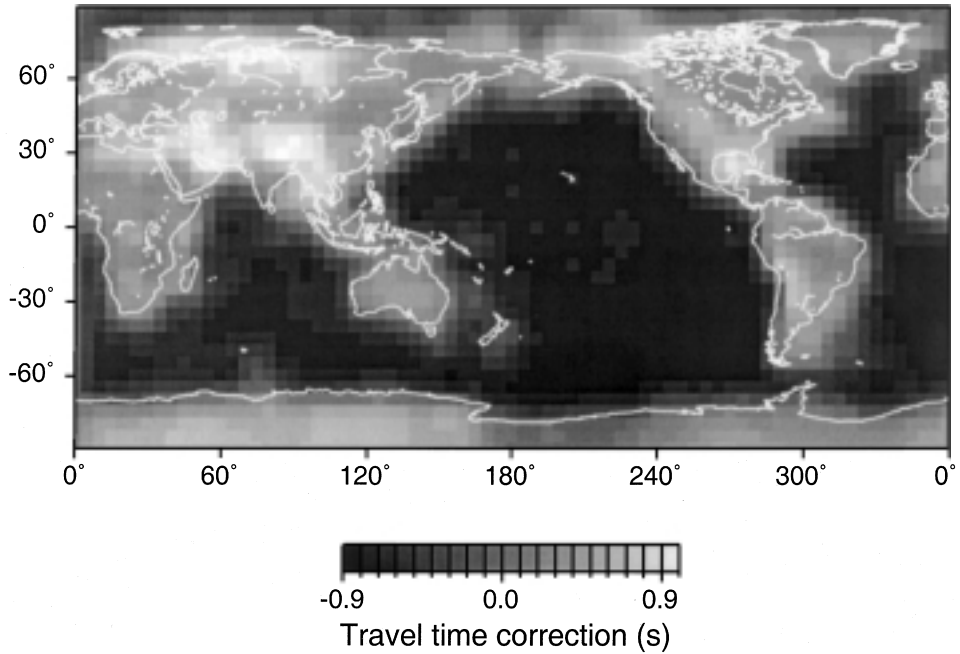
Figure 1

One-way travel-time corrections (relative to PREM crust) for a *P* wave in model CRUST5.1 of MOONEY *et al.* (1998). Vertical incidence is assumed at the base of the crust.

of ENGDAHL *et al.* (1998) in each of the *i* source bins, and the correction for each bin is then

$$S^{ij} = \frac{1}{K} \sum_{k}^{K} t_r^{ijk} \tag{2}$$

where the travel-time residual after relocation is

$$t_r^{ijk} = [t_{\text{obs}} - (t_o + \delta t_M + \delta t_C + \delta t_E + \delta t_{EL})]^{ijk}. \tag{3}$$

The superscript *j* refers to the station and the sum is over each *k* event within the source bin, t_o is the reference model travel time, δt_C is the crustal correction for the raypath, δt_E is the ellipticity correction and δt_{EL} is the elevation correction. Thus, the station corrections incorporate local site effects as well as unmodeled mantle or crustal structure which might produce similar delays at nearby stations. In theory, it would seem preferable to calculate corrections for bins which are as small as possible. However, it is unclear whether there are enough data currently available to constrain region-dependent corrections for many stations. We have arbitrarily employed a cutoff for each source bin of four observations; if a bin contains fewer events for any

particular station the correction term is set to zero. All of the station corrections were calculated using CRUST5.1 as the crustal model. We used these station corrections in the analysis using the full data set.

Figure 2 compares corrections for station JAS in California and models SP12 and BDP98. Many areas exhibit strong correlation in the corrections between adjacent bins, indicating significant unmodeled structure. However, the mean value of the corrections is quite small, on the order of 0.1 s. In some areas (South America and the Caribbean) the corrections vary considerably within a short distance, and
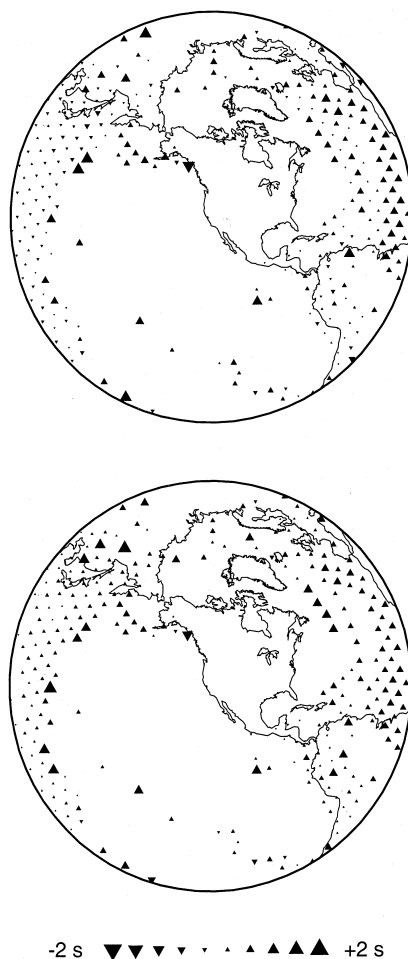

Figure 2
Station correction terms for station JAS in California plotted at the center of 5° × 5° equal-area bins. The top map shows corrections calculated for model SP12 and the lower map for model BDP98. The overall pattern and amplitude of the corrections are very similar for both models.
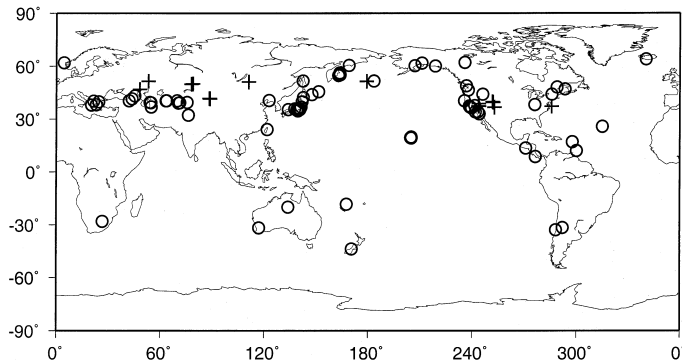
Figure 3
Locations of test events used in this study. Explosions are indicated by crosses and earthquakes by circles. Epicentral information is listed in SMITH and EKSTRÖM (1996) and KENNETT and ENGDAHL (1991).

probably are determined largely by structure near the particular source bins. The corrections are similar for both models and are dominantly positive. This indicates the presence of additional slow anomalies, probably in the upper mantle under JAS, which are not completely compensated for in either model.

Relocation Method

Each event is relocated by standard nonlinear least-squares, with the depths held fixed at the surface for explosions and at the depth reported in KENNETT and ENGDAHL (1991) for the earthquakes, owing to the lack of depth resolution of teleseismic *P* waves. Since the change in epicentral location is small during the inversion, the 3-D mantle correction calculated for the initial location, that of the ISC, is used throughout. When we tested the effect of varying the 3-D mantle corrections between iterations for model SP12, the average difference in location for the test events was ~0.2 km.

The inversion process continued until the root-mean-square of the weighted travel-time residuals changes by less than 0.001 s, usually in 3–5 iterations. Weighting was assigned to the residuals in the following manner:

$$w = 1.0, \quad Z < 3.333$$
$$w = e^{-(0.3*Z)^2-1}, \quad 3.333 < Z < 20.0 \tag{4}$$
$$w = 0.0, \quad Z > 20.0$$

where $Z = |\bar{t} - t_r|$. $\bar{t}$ is the mean travel-time residual in the azimuthal quadrant of the observation. This type of weighting scheme was used in order to include residuals in the inversion which are large due to a poor initial location.

Analysis

Full Data Set

The results of relocating all of the test events using the complete set of ISC teleseismic *P* waves, and without empirical station corrections, are summarized in Table 1. As was found by SE96, there is a considerably better improvement in locations of the explosions than the earthquakes relative to PREM, however for these results the improvement in the earthquake locations is greater. This is probably due to the fact that we have used a smaller distance cutoff than that used by SE96, which only inverted data recorded at distances larger than $30°$. The most striking aspect of these results is that model SP12 generates the smallest mislocations for both earthquakes and explosions. The rms mislocation for this model is about 2 km smaller than that using the other 3-D models. As mentioned above, model MK12, although it has the same parameterization as SP12, was originally derived as a model of bulk sound and shear velocity. Thus, we might expect this model to provide a smaller improvement in event location when using only *P* waves. The other two models (BDP98 and VWE97), however, are block models with nominally higher resolution and were constructed using only *P* wave (also *pP* for VWE97) travel-time residuals. VWE97 contains the most free parameters of the 3-D models. The performance of these two models relative to SP12 is therefore somewhat surprising.

Table 1 suggests that appropriate correction for crustal structure is just as important as the choice of 3-D mantle model. Not surprisingly, we observe a large improvement in location quality using the full CRUST5.1 model over the rather crude crustal correction employed by Su *et al.* (1994). This is especially true for the explosion events where this improvement is equal to that of using SP12 over the other mantle models. The rather coarse parameterization of CRUST5.1 may be a factor in the small improvement observed for the earthquakes, since many of these events

Table 1

Root-mean-squares mislocation in km for earthquakes and explosions using a particular velocity model and all available teleseismic P phases.

Model	Explosions	Earthquakes
PREM + C5.1	12.92	18.83
SP12 + OCF	8.47	15.57
SP12 + C5.1	7.83	15.37
MK12 + OCF	11.14	17.92
MK12 + C5.1	9.53	17.40
BDP98 + OCF	11.43	17.22
BDP98 + C5.1	9.80	17.13
VWE97 + C5.1	10.51	17.33

OCF refers to use of the ocean-continent function crustal corrections, C5.1 to the use of the CRUST5.1 model.

occur along coastlines where the crustal thickness varies rapidly over short distances. Nevertheless, this model is quite effective in reducing much of the regional bias in *P*-wave travel times due to crustal structure.

Mislocation vectors for the test events in models SP12 and and BDP98 are compared in Figure 4. The considerably smaller location errors for explosion events, even compared with earthquakes located nearby, is obvious. The general trend for location errors using BDP98 to be larger than those using SP12 exists for all regions. Locations derived from BDP98 are generally displaced from the true location in the same direction as those derived from SP12, although by longer distances. This suggests that the amplitudes of large velocity anomalies are not as well recovered in BDP98, although the lateral positions of the anomalies are similar to SP12.
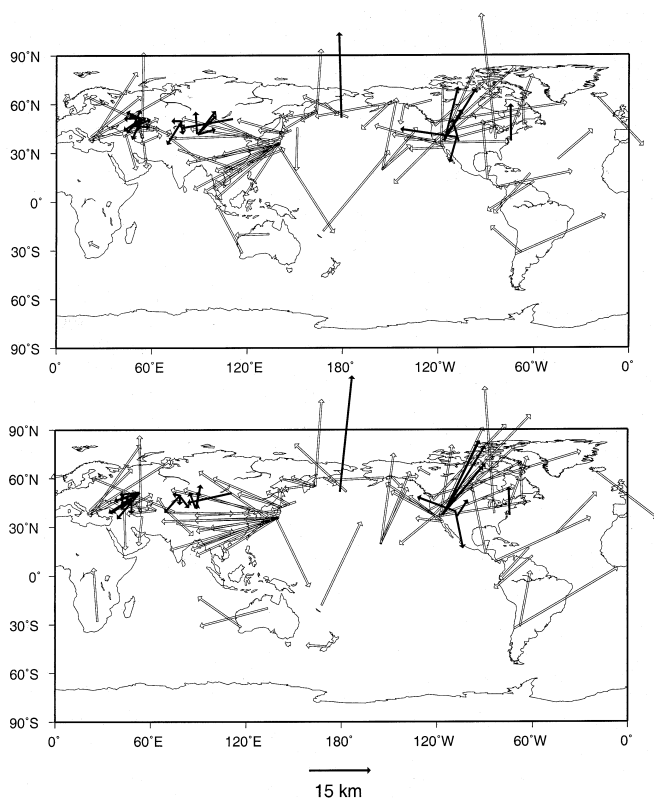

Figure 4
Mislocation vectors for the test events using the complete ISC *P*-wave travel time set, for models SP12 (*top*) and BDP98 (*bottom*) without station corrections. Length of the vectors is proportional to the magnitude of the mislocation. The base of each arrow is plotted at the ground-truth location and each vector points in the directon of the model-derived location. Explosion events are plotted as the solid vectors and earthquakes as the open vectors. Events located with BDP98 are generally mislocated in the same direction as with SP12, but with a larger error.

One area in which the location difference between BDP98 and SP12 is especially large is in the western United States. It is interesting to compare residuals predicted for these two models for events in this region. Although the areas for which the two models predict particularly large residuals are similar (Fig. 5), in general the amplitudes of the residuals predicted by SP12 are larger. The residual pattern predicted by SP12 markedly better matches the wide variation in the observed residuals (Fig. 6). In contrast, the residuals predicted by both models for events at the Semipalatinsk nuclear test site are notably more similar, although differences (notably in North Africa and Australia) do exist. As a result the locations derived from both models for events in central Asia are quite similar.

One expected result of using 3-D models containing larger numbers of free parameters is a better fit to the travel times. Figure 7 shows the rms residual obtained for the test events using each of the 3-D models. SP12 and MK12 produce similar
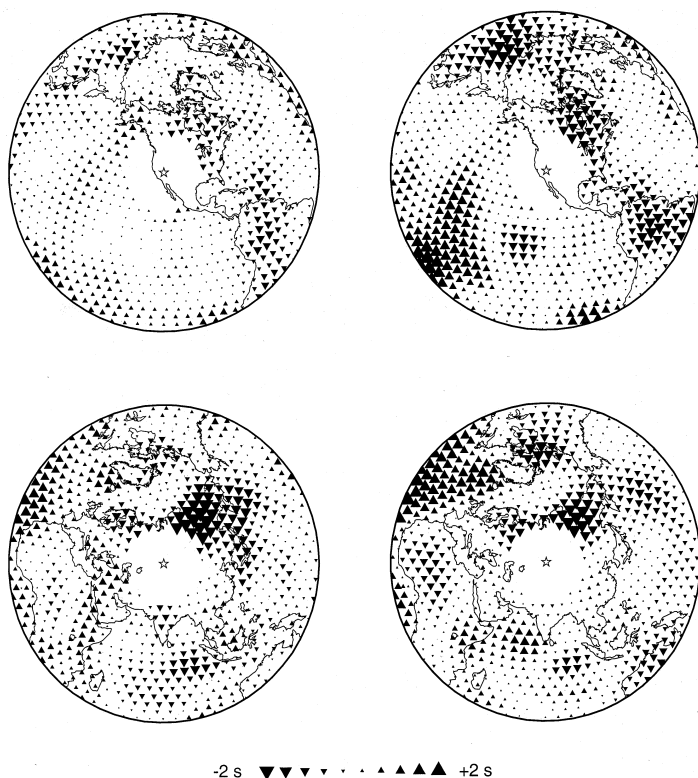

-2 s ▼ ▼ ▾ · · ▴ ▲ ▲ +2 s

Figure 5

Predicted travel-time residuals plotted in 5° × 5° bins for models BDP98 and SP12 for events located at the Nevada and Semipalatinsk nuclear test sites. Each triangle represents the value of the mantle travel-time correction in the center of the bin after removal of the mean value over all bins. Top two maps are for an event at the Nevada test site and the bottom two maps are for an event at the Semipalatinsk test site. Maps on the left are for BDP98 and those on the right are for SP12.
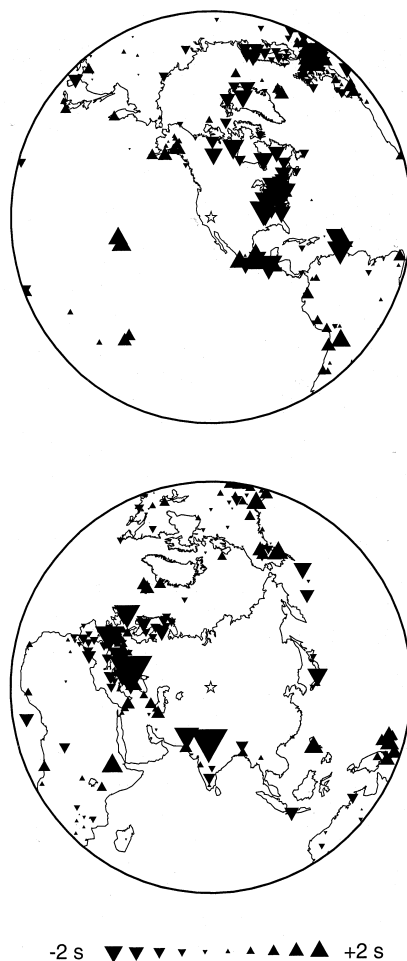
Figure 6

Mean observed *P*-wave travel-time residuals for explosions at the Nevada (*top*) and Semipalatinsk (*bottom*) test sites. The value plotted is the difference between the observed travel time and the value predicted for PREM plus all additional corrections except for the mantle correction. The mean of all of the values has been subtracted from each data point. Residuals with a magnitude larger than 5 s have been excluded.

magnitude residuals, whereas the rms residual for the block models is 0.3–0.4 s smaller. We also note that the origin times are on average better fits using the block models, yet the block models do not improve the fit to the location parameters over the other models. Smaller residuals alone should not be taken as an indication of the reliability of locations.

We then applied the empirical station corrections described above in the locations. Table 2 lists the average mislocation obtained for all test events, using three types of station corrections as well as no station corrections. The station
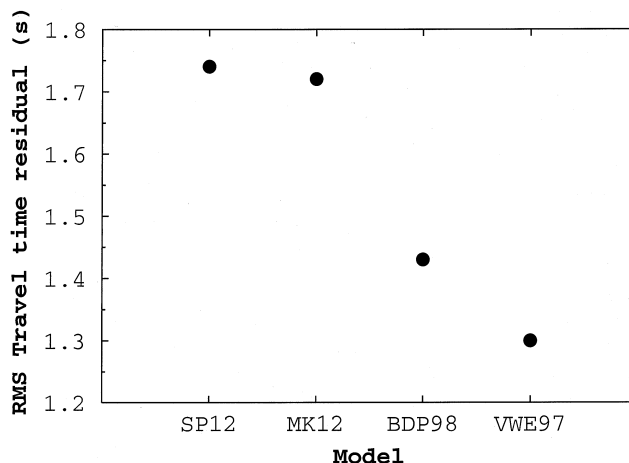
Figure 7

The rms travel-time residual remaining after relocation of the test events using each of the 3-D models and all available phase observations. The mean value was removed from each residual before calculating the rms. The rms residual values for the two models parameterized by blocks (BDP98 and VWE97) are significantly smaller than for the other two models.

Table 2

Average mislocation in km for all events using various types of station corrections.

Model	No corrections	Invariant corrections	5° bins	2.5° bins
SP12	11.71	12.22	11.75	11.73
MK12	13.11	13.58	13.12	13.09
BDP98	13.06	13.46	13.09	13.06
VWE97	13.72	14.07	13.73	13.69

Bins for source region-dependent corrections are either 5° (column 4) or 2.5° (column 5) wide in epicentral distance.

correction terms are in addition to the corrections for the 3-D model and the crust. The third column of Table 2 displays results obtained when station corrections which are not dependent on the source region of the event are used. The last two columns list the average mislocation obtained when the station corrections are calculated using source bins with a width of 5° in azimuth and either 5° or 2.5° in epicentral distance from each station. The bins are non-overlapping.

The invariant station corrections produce mislocations which are consistently larger for all 3-D models. It is quite clear that mixing correction terms for events in all source regions is not appropriate. Somewhat better results are found when using the region-dependent corrections. However, the improvement in the average

mislocation is still negligible. This is most likely due to the fact that for only a fraction of the phases used for each event is there enough information to constrain the station correction term. As mentioned above, the correction term was set to zero if there are fewer than four events located within the source bin. The results listed in Table 2 were obtained utilizing all available *P* waves, regardless of whether a station correction term was available. For most of the events, there are insufficient stations with nonzero correction terms to significantly affect the location error. The lack of improvement may also result because most of the unmodeled structure is removed through the crustal correction. A third possibility is that the application of corrections which vary in such a rough manner is not appropriate, and that applying smooth function to the correction values may result in greater improvement to the locations, much in the manner of SCHULTZ *et al.* (1998).

Somewhat better results are obtained when restricting the data set to only those stations with nonzero correction terms. In this case, using the region-dependent correction terms and restricting the analysis to only those events with 20 or more such stations, the average mislocation is improved by about 0.5 km. The results are similar for all of the 3-D models.

Figure 8 suggests that significant improvement in location accuracy over that enabled by current 3-D models may only be achieved by taking into account structure very local to the source. We calculated "site-specific" station corrections for a group of explosions in the western U.S. and a group in central Asia. One event from each group was selected as a reference event which was relocated using model SP12 and the resulting residual taken as the correction for each station. Figure 8 shows the relocations obtained for both groups of events both with and without these corrections. This procedure resulted in significant improvement in location accuracy for those events located within 50 km of the reference event but degraded the accuracy for events only slightly more distant. Further reduction of the source bin sizes for the purpose of calculating empirical station corrections would thus be desirable although there is not enough phase data available in current event bulletins to make such an effort fruitful.

Sparse Data Sets

As noted above, it is important to examine the performance of 3-D models when locating events teleseismically with a limited number of phases. The primary seismic network of the International Monitoring System, for example, is to consist of only 50 3-component stations and arrays worldwide. Station coverage in many areas is therefore sparse. In this section we discuss location experiments using only subsets of the available *P*-wave data set.

For each of the test events we randomly selected 30 of the available phases and relocated the event according to the procedure described above. We repeated this
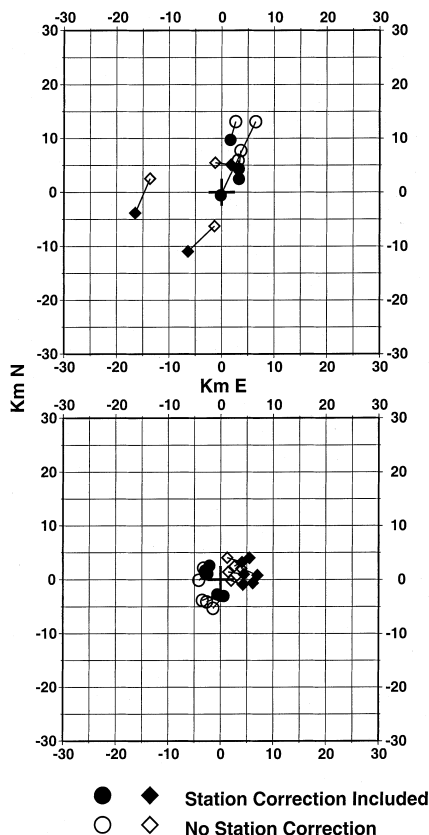
Figure 8

Map grids showing relocation of explosions using site-specific station corrections. Top map shows relocation of explosions in the western U.S. and the bottom map from the former Soviet Union. In each case, a set of station corrections was computed applying the residuals resulting from relocation of one of the events in model SP12. Test events in the same region were then relocated both with (closed symbols) and without (open symbols) these station correction terms. Circles correspond to those events located in the immediate vicinity (within 50 km) of the reference events, while the diamonds correspond to events located up to 5° distant. The ground-truth location for each event is assumed to be at the cross located in the center of the grid. In each case the location accuracy obtained for the closer events is improved while that for the more distantly located events is degraded.

procedure 100 times for each event. No consideration with regard to the azimuth or epicentral distance of the reporting station was made when selecting the phases, except that the distance was restricted to between 25° and 96° as before. A location trial is deemed to be "successful" if it results in a location within the 1000 km^2 circular area surrounding the actual location specified by the CTBT. Formal calculation of error ellipses often results in areas of less than 1000 km^2 uncertainty which may not include the ground-truth epicenter. However, for the purposes of the CTBT, the area set aside for on-site inspection would include the actual epicenter in these cases.

In addition to relocating the events in this manner using only the model travel-time corrections, we also computed new station corrections using only the set of test events. We divided the test events into groups containing three or more events, and from each group selected a reference event, usually the event with the largest number of recorded phases. Each group consisted of events located 500 km or less from the reference events. We then take as the station correction the residual remaining after relocation of the reference event in the 3-D model. These corrections are referred to as ''model-based'' corrections. Station corrections were also calculated using the ground-truth location for each event and are referred to as ''ground-truth'' corrections. This procedure was thus similar to that described in Figure 8 except that we limited the available phases to only those with a nonzero correction (i.e., to those stations recording the reference event). However, since the stations reporting nearby test events are similar, most of the available stations have a correction for a given event. This procedure allowed computation of station corrections for 69 of the total of 112 test events.

Figure 9 presents the results of this process for an explosion in the Ural mountains. Results of location trials using model SP12 are compared with those using PREM. Each closed circle is the result of one location trial using 30 *P*-wave phases, and the model used in the relocations is displayed at the top of the appropriate map. For the top two panels in Figure 9, we used no station corrections in addition to the models indicated. The two bottom grids depict results using SP12 and either the model-based or the ground-truth station corrections. Each level of complexity in the model which is employed results in better locations. For PREM the average location error is about 10 km and about 5 km for SP12. Using SP12, most of the location trials lie within the 1000 km^2 objective of the CTBT. The use of station corrections aids removal of both the scatter and the bias in the location trials.

Results of the location trials are displayed geographically in Figures 10–14 for the four 3-D models and for PREM. The top map in each figure displays the percentage of the location trials which satisfies the CTBT objective for the trials using 30 phases without station corrections. The bottom map displays the same for trials with use only 8 phases from each event (250 trials per event). As can be seen from these figures, the quality of the locations seems to vary randomly with geographic location. Events in central Asia are consistently well-located, with generally above 60% of the location trials satisfying the treaty criterion. Most of these events are explosions. The areas showing particularly less satisfying results are western North America (including the Nevada Test Site explosions) and southern Europe. Again these maps suggest a large effect resulting from structure close to the sources, as the results are often quite different for events located near to each other.

Results for three of the four 3-D models are quite similar and provide noticeable improvement over PREM in most areas. Model VWE97 gives fewer successful trials than the other 3-D models. The percentage of successful trials is, however, considerably degraded using only 8 phases. Few of the events have as many as
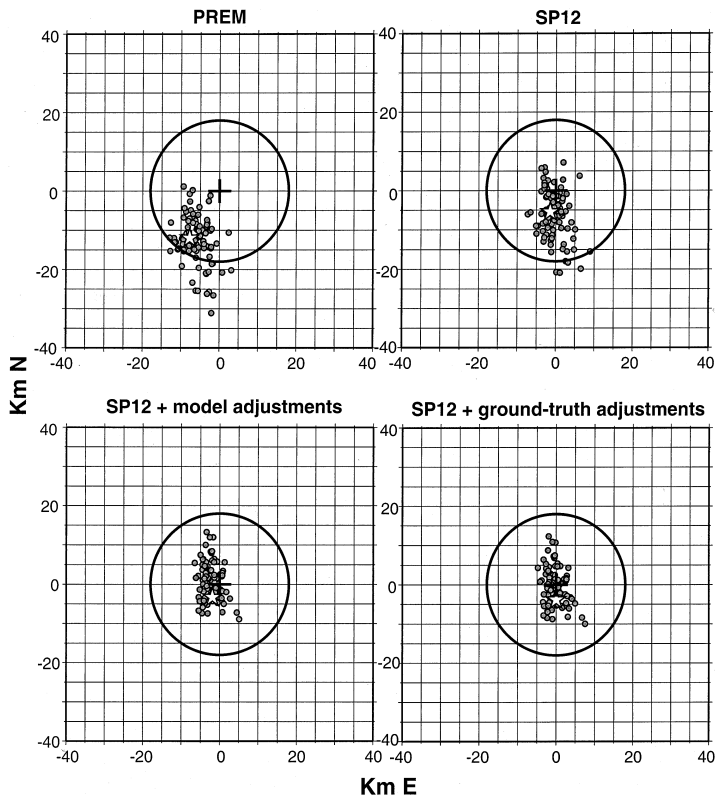
Figure 9
Results of 100 location trials, each using only 30 *P*-wave observations, for a single explosion located near the southern Ural mountains. Each grid is a map-view with the ground-truth location denoted by the black cross at the center. The velocity model used for each set of trials is shown at the top of the grid. The grid at top left is for PREM with no station corrections; that at the top right for SP12 with no station corrections; the lower-left grid is for SP12 with model-based station corrections; and the lower-right grid is for SP12 with ground-truth corrections. Each filled circle depicts the location resulting from one of the trials. The white stars indicate the locations obtained from all available phases. The black circles delineate an area of 1000 km² surrounding the ground-truth location.

60% of the location trials which satisfy the treaty criterion regardless of the model used.

The breakdown of the location trials is summarized by Tables 3 and 4 and Figure 15. When using no station corrections and 30 total phases, the percentage of successful trials is 65–70%, and the average mislocation is only slightly greater than that obtained using all phases (Table 2). The model-based station corrections produce improvement in the average mislocation although not in the number of successful trials. The ground-truth corrections produce significant improvement in both average location and percentage of successful trials. If ground-truth information is available, then an event can be located at a confidence level of
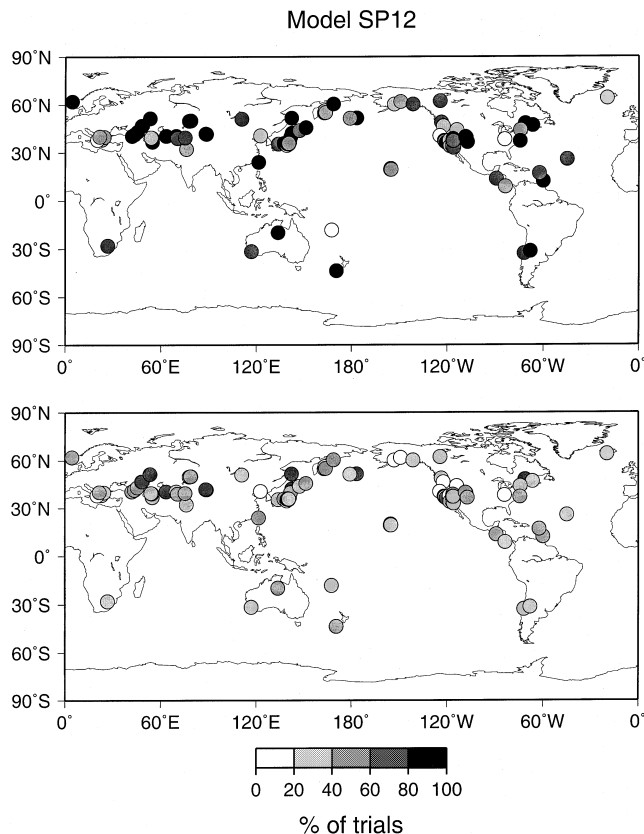
Figure 10
Maps showing the percentage of trials resulting in a location within an area of 1000 km² about the ground-truth location for each of the test events. The degree of gray-shade for each event is proportional to the number of successful trials. The top map is for the trials using 30 phases and the bottom map for those using 8 phases. The model used was SP12 with the CRUST5.1 crustal corrections and no empirical station corrections.

75–80% within the goal of the CTBT. This is even true when using PREM as the location model, which points to the importance of calibration information, if available. The ground-truth corrections reduce the difference between the results for the different models. If only 8 phases are used in the inversion, fewer than half of the trials are successful and the average mislocation exceeds 30 km for all the 3-D models.

Figure 15 displays the number of trials with location errors in 5-km bins as well as greater than 20 km. Again, the distribution of the location trials is similar for three of the 3-D models with VWE97 resulting in slightly larger errors. Use of ground-truth information results in ~50% of the trials yielding a location error of less than 10 km (with 30 phases). In this case, the distribution of the location errors using PREM is
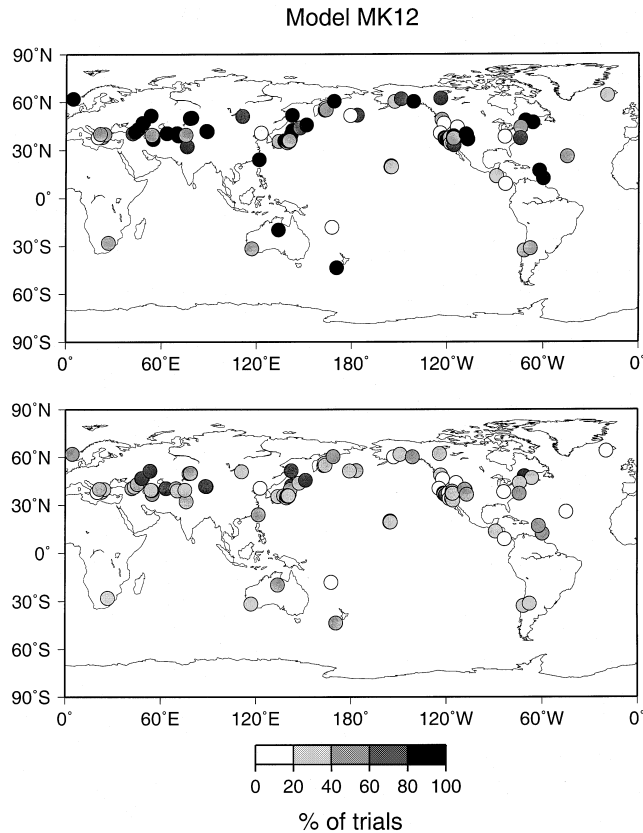
Figure 11
Similar figure to Figure 10 using model MK12.

almost exactly the same as using one of the 3-D models. In the absence of calibration information, however, the quality of the locations derived from the 3-D models is clearly superior. Without station corrections, the median mislocation is roughly 12 km using 30 phases, and 20 km using 8 phases.

Discussion

Enough data seem to be currently available to conclude that, while all 3-D models of mantle velocity seem to provide substantial improvement over 1-D models in the ability to locate teleseismic events, the degree of improvement does not necessarily increase with the complexity of the model. Since it appears that neither the parameterization chosen for the tomographic inverse problem, nor the particular inversion technique used greatly affect the solution obtained (BOSCHI
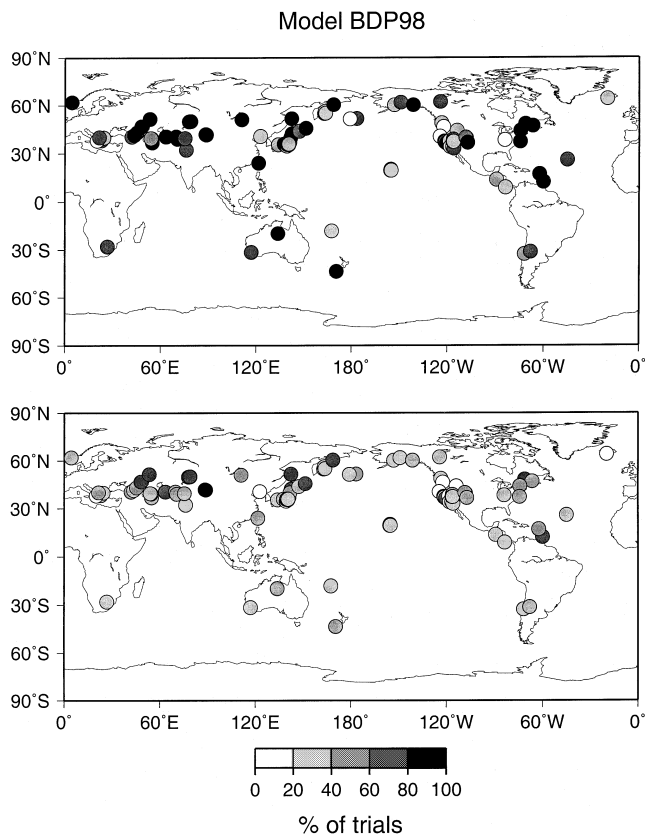
Model BDP98

Figure 12
Similar figure to Figure 10 using model BDP98.

and DZIEWONSKI, 1999a), an alternative explanation for this result should be invoked. For example, the type of regularization and damping employed in the inversion for block models with nonuniform data coverage might result in substantially lower amplitude anomalies in regions where the coverage is relatively low. This might lead to a tendency for block models to underpredict the range of observed residuals for events in some regions, such as we observe in Figure 5.

Another possibility which requires full investigation is the effect of multiple data sets to constrain the *P*-wave velocity in the mantle. Many spherical harmonic models of mantle velocity such as SP12 and MK12 have been obtained using a variety of absolute and differential times as well as waveform data. However, present limitations of computer memory prevent the use of such large data sets when inverting for models of high resolution. *P*-wave travel times are largely sensitive to structure in the mid- and lower mantles whereas the combination of travel times and
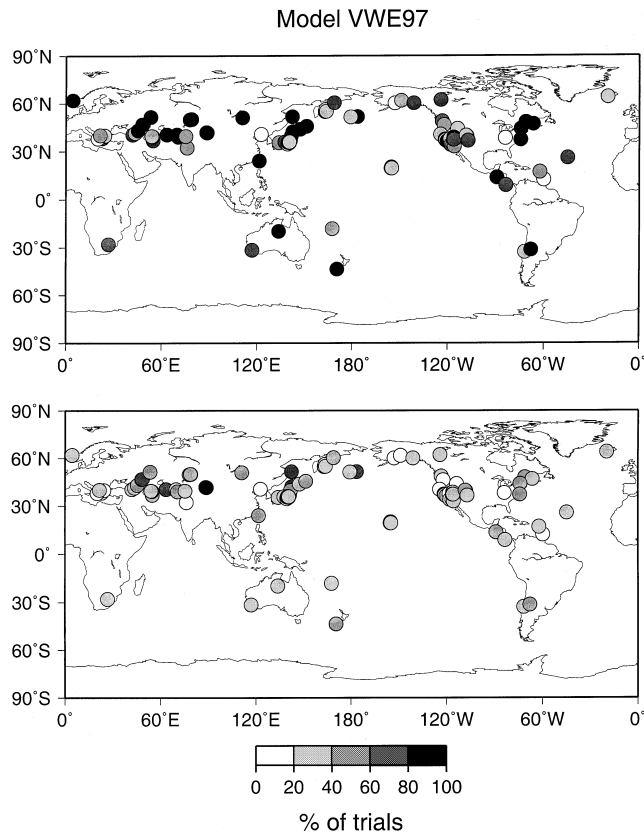
Figure 13
Similar figure to Figure 10 using model VWE97.

waveforms may lead to more even resolution with depth. Nevertheless, it would seem rather unlikely that the phases recorded for the test events used here are overly sensitive to areas of the mantle where resolution is relatively poor for the two block models. Most of the events occur in regions where nearby seismicity is relatively abundant.

The fact that the block models produce substantially better fits to the ISC residuals, while failing to improve the quality of teleseismic locations, also brings into question the quality of the data, particularly in the early years. The effect of poor phase picks may limit the ability to accurately locate events and the production of more detailed models for this purpose may prove futile. The mapping of earthquake mislocations into the production of tomographic models therefore probably does not decrease with increasing model complexity.

To some extent, the results from the location trials with sparse data sets are encouraging in that small to moderate teleseismic events may be located to within the
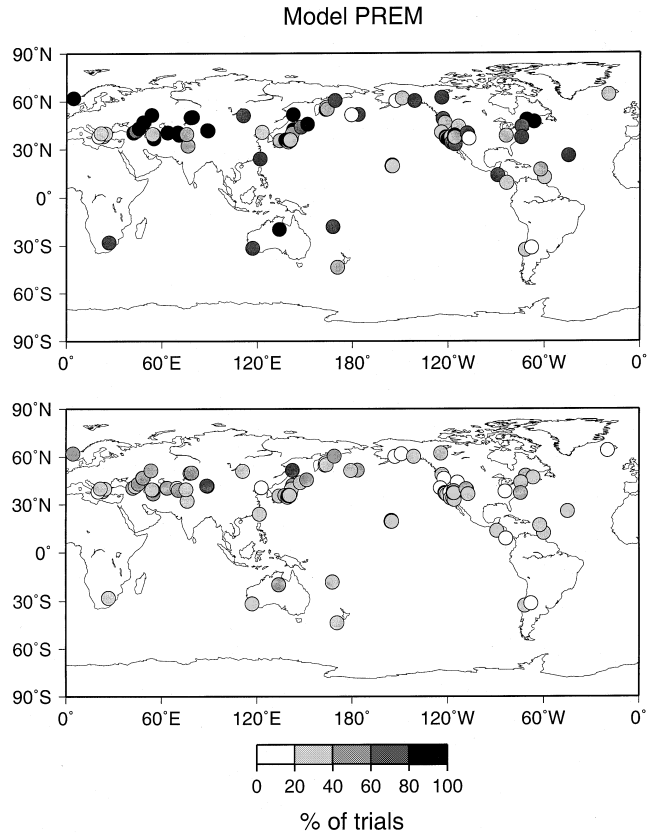
Model PREM

Figure 14
Similar figure to Figure 10 using PREM.

Table 3

Average mislocation in km for location trials using a random selection of 30 phases. 100 trials were computed for each event.

Model	No corrections	Model-based corrections	Ground-truth corrections
SP12	14.32 (71.5%)	13.74 (70.8%)	11.02 (79.1%)
MK12	15.24 (67.7%)	14.30 (68.3%)	10.97 (78.8%)
BDP98	14.80 (69.3%)	14.27 (68.8%)	10.79 (79.6%)
VWE97	16.49 (64.9%)	16.11 (64.2%)	11.88 (75.8%)
PREM	17.42 (61.8%)	…	11.23 (78.8%)

See text for description of station corrections. Numbers in parentheses are the percentage of location trials falling within a circular area of 1000 km^2 surrounding the ground-truth location.

specified 1000 km^2 area for the CTBT about two-thirds of the time. The median mislocation in such circumstances is around 12 km. This is true even if calibration information is not available for any of the stations. Further improvement may be

Table 4

Average mislocation in km for location trials using a random selection of 8 phases. 250 trials were computed for each event.

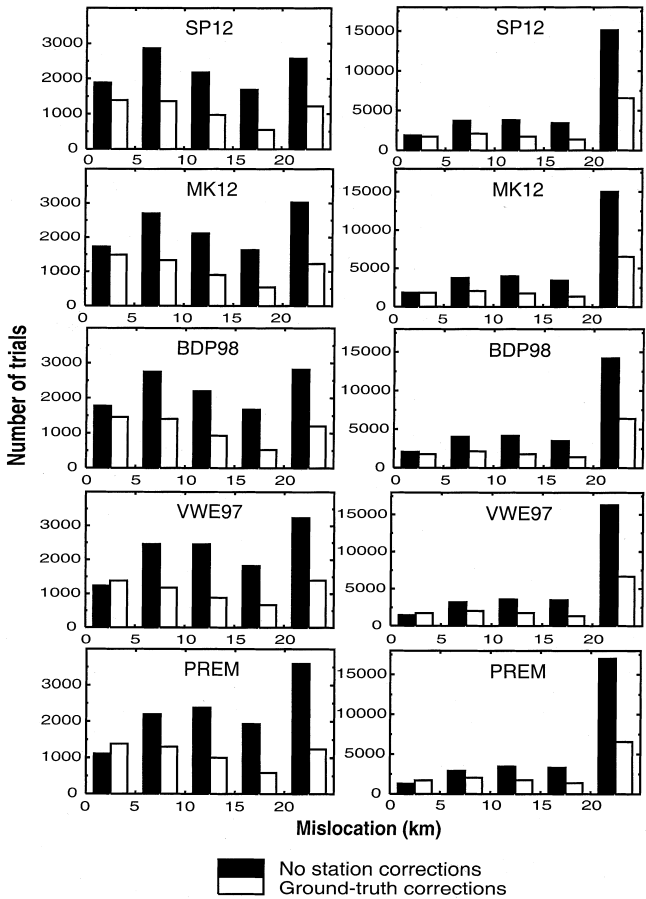| Model	No corrections	Model-based corrections	Ground-truth corrections
SP12	38.79 (41.3%)	33.10 (52.7%)	31.06 (56.6%)
MK12	36.90 (41.9%)	32.74 (52.4%)	32.50 (57.3%)
BDP98	33.87 (44.5%)	31.10 (52.8%)	28.62 (58.3%)
VWE97	37.81 (36.9%)	32.65 (49.2%)	29.26 (56.4%)
PREM	42.57 (34.6%)	…	29.16 (56.8%)

Figure 15

Histograms depicting the distribution of location errors for the trials using 30 phases (*left*) and 8 phases (*right*) for all the 3-D models and for PREM. The height of each bar represents the number of location trials resulting in a mislocation within a 5-km wide bin, except that the last bin contains all location trials with a mislocation larger than 20 km. Filled bars show results for location trials using no empirical station corrections while the open bars are for the trials using the ground-truth corrections. The open bars do not include results for the reference events used to calculate the ground-truth corrections.

possible if care is taken to ensure that sufficient observations are used from all azimuthal quadrants, which we have not done in this study. The probability of achieving this accuracy is increased to over 75% if calibration information is available.

On the other hand, for very small events only a handful of observations may be available. In such cases it probably will be impossible to achieve adequate azimuthal coverage. The results demonstrate that calibration information is essential if one is to achieve the desired accuracy with a confidence level of even 50%. For these events the addition of regional phases is likely to be essential, which places importance on accurate mapping of P_n velocities (e.g., SMITH and EKSTRÖM, 1999). Due to their frequency content and low background noise level, first-arriving P waves are likely to remain the most useful data for teleseismic event location, although S waves, pP and core phases provide important constraints on depths (ENGDAHL *et al.*, 1998). The use of azimuth data may hold further promise. Such data are already used by the Prototype International Data Center in producing their event bulletin (BONDÁR *et al.*, 1998) and have already been shown to substantially improve the accuracy of regional locations [DREGER *et al.*, 1998; BRATT and BACHE, 1988). Three-dimensional models may be used to provide corrections for the azimuth data in the absence of calibration information for certain stations.

Accurate corrections for crustal structure are seen to considerably improve prospects for teleseismic event location. Further improvement and refinement of existing crustal models is certainly desirable and may in the future lessen the need for empirical station corrections to teleseismic phases. Based on Figure 2, it is likely that most of the unmodeled structure resides in the crust and upper mantle directly beneath the station. In this regard, we also believe that the incorporation of anisotropy into 3-D tomographic modeling may further improve the utility of teleseismic P waves in event location (BOSCHI and DZIEWONSKI, 1999b). Both the upper mantle (e.g., BEGHOUL and BARAZANGI, 1990; SMITH and EKSTRÖM, 1999) and perhaps the area near the CMB likely contains P-wave anisotropy on the order of several percent, however its nature and how it is best parameterized in tomographic modeling is as yet unclear.

Conclusions

In summary, we have used a data set of explosions and earthquakes with well-known locations to test the accuracy of teleseismic event locations obtained using four different 3-D models of P-wave velocity in the mantle. The 3-D models include two parameterized horizontally in terms of spherical harmonic functions reaching degree 12 and two which are represented in terms of constant velocity blocks. Thus the latter two models provide better horizontal resolution. However, the two block models do not improve upon the accuracy of the locations. Using all the available

teleseismic *P*-wave observations in the ISC catalog, the average mislocation obtained for the test events using the two block models is 2–3 km larger than the best of the spherical harmonic models, model S&P12/WM13 of Su and Dziewonski (1993). This occurs despite the fact that the block models provide a better fit to the travel times. From analysis of the mantle corrections to the travel times, it appears that existing block models may underestimate the amplitudes of long-wavelength travel-time anomalies.

The largest effect on the accuracy of the locations appears to originate from structure in the crust or upper mantle near the sources. Use of the crustal model of Mooney *et al.* (1998) to correct travel times on both the source and receiver side results in a large reduction in the mislocation over an earlier, less detailed crustal model. Source-region dependent station corrections calculated for the 3-D models have little effect on the locations unless the source bins are very small (much less than 5° in dimension). Current event bulletins probably do not contain enough data to adequately constrain empirical corrections in such small bins, so as to significantly improve upon locations derived from mantle 3-D models and crustal corrections.

In the second half of the paper we tested the ablity of the 3-D models to provide accurate locations for small to moderate events recorded by only a limited number of phases. For each of the test events we performed 100 separate location trials applying a different random selection of 30 phases and 250 separate trials using 8 phases. Again, the block models do not improve the outcome of the trials over the spherical harmonic ones. Using 30 phases, approximately two-thirds of the trials result in a location within the $1,000 \text{ km}^2$ area specified for on-site inspection under the CTBT. This percentage decreases to less than half using only 8 phases. If ground-truth information is available to correct the travel times, however, the percentage of trials which result in a location within the specified area is some 79% and and 57% using 30 and 8 phases, respectively. Adopting PREM to locate the test events along with ground-truth calibration is equally effective as using any of the 3-D models. At present, however, ground-truth information is available for only limited regions of the globe and for seismic stations that have remained in extended operation.

Acknowledgements

References

Bratt, S. R., and Brache, T. C. (1988), *Locating Events with a Sparse Network of Regional Arrays*, Bull. Seismol. Soc. Am. *78*, 780–798.

Beghoul, N., and Barazangi, M. (1990), *Azimuthal Anisotropy of Velocity in the Mantle Lid beneath the Basin and Range*, Nature *348*, 536–538.

Bondár, I., Yang, X., Wang, J., Bahavar, M., Israelsson, H., and McLaughlin, K., *Tuning and calibration activities at the PIDC*, Proc. 20th Annual Seismic Res. Symp. on Monitoring a Comprehensive Test-Ban-Treaty, Santa Fe, NM (J. Fantroy *et al.*, eds.) 1998, 1–10.

Boschi, L., and Dziewonski, A. M. (1999a), *High and Low-resolution Images of the Earth's Mantle: Implications of Different Approaches to Tomographic Modeling*, J. Geophys. Res. *104*, 25,567–25,594.

Boschi, L., and Dziewonski, A. M. (1999b), *Whole Earth Tomography from P, PcP, and PKP Delay Time Measurements: The Possibility of Laterally Varying Radial Anisotropy Throughout the Mantle*, EOS *80*, S13.

Dziewonski, A. M. (1984), *Mapping the Lower Mantle: Determination of Lateral Heterogeneity in P Velocity up to Degree and Order 6*, J. Geophys. Res. *89*, 5929–5952.

Dreger, D. S., Uhrhammer, R., Pasyanos, M., Franck, J., and Romanowicz, B. (1998), *Regional and Far-regional Earthquake Locations and Source Parameters Using Sparse Broadband Networks: A Test on the Ridgecrest Sequence*, Bull. Seismol. Soc. Am. *88*, 1353– 1362.

Ekström, G., Dziewonski, A. M., and Smith, G. P. (1997), Strategies for improving seismic event location at regional and teleseismic distances. In *Proc. 19th Annual Seismic Res. Symp. on Monitoring a Comprehensive Test-Ban-Treaty* (M. J. Shore *et al.*, eds.) 221–229.

Engdahl, E. R., van der Hilst, R. D., and Buland, R. P. (1998), *Global Teleseismic Earthquake Relocation with Improved Travel Times and Procedures for Depth Determination*, Bull. Seismol. Soc. Am. *88*, 722–743.

Grand, S. P., van der Hilst, R. D., and Widiyantoro, S. (1997), *Global Seismic Tomography: A Snapshot of Convection in the Earth*, GSA Today *7*(4), 1–7.

Jeffreys, H., and Bullen, K. E., *Seismological Tables* (British Association for the Advancement of Science, London, 1958).

Kennett, B. L. N., and Engdahl, E. R. (1991), *Travel Times for Global Earthquake Location and Phase Identification*, Geophys. J. Int. *105*, 429–465.

Kennett, B. L. N., Engdahl, E. R., and Buland, R., (1995), *Constraints on Seismic Velocities in the Earth from Travel Times*, Geophys. J. Int. *122*, 108–121.

Li, X., and Romanowicz, B. (1996), *Global Mantle Shear Velocity Model Developed Using Nonlinear Asymptotic Coupling Theory*, J. Geophys. Res. *101*, 22,245–22,272.

Mooney, W. D., Laske, G., and Masters, T. G. (1998), *CRUST 5.1: A Global Crustal Model at $5° \times 5°$*, J. Geophys. Res. *103*, 727–747.

Schultz, C. A., Myers, S. C., Hipp, J., and Young, C. J. (1998), *Nonstationary Bayesian Kriging: A Predictive Technique to Generate Spatial Corrections for Seismic Detection, Location, and Identification*, Bull. Seismol. Soc. Am. *88*, 1275–1288.

Smith, G. P., and Ekström, G. (1996), *Improving Teleseismic Event Locations Using a Three-dimensional Earth Model*, Bull. Seismol. Soc. Am. *86*, 788–796.

Smith, G. P., and Ekström, G. (1999), *A Global Study of P_n Anisotropy beneath Continents*, J. Geophys. Res. *104*, 963–980.

Su, W., and Dziewonski, A. M. (1993), *Joint 3-D Inversion for P and S Velocity in the Mantle*, EOS *74*, 557.

Su, W., Woodward, R. L., and Dziewonski, A. M. (1994), *Degree-12 Model of Shear Velocity Heterogeneity in the Mantle*, J. Geophys. Res. *99*, 6945–6980.

Su, W., and Dziewonski, A. M. (1997), *Simultaneous Inversion for 3-D Variations in Shear and Bulk Velocity in the Mantle*, Phys. Earth Planet. Inter. *100*, 135–156.

van der Hilst, R. D., Widiyantoro, S., and Engdahl, E. R. (1997), *Evidence for Deep Mantle Circulation from Global Tomography*, Nature *386*, 578–584.

VASCO, D. W., and JOHNSON, L. R. (1998), *Whole Earth Structure Estimated from Seismic Arrival Times*, J. Geophys. Res. *103*, 2633–2671.

WALLACE, T. C., and TINKER, M. A. (2001), *Locations and Yields of Lop Nor Underground Nuclear Explosions*, Pure appl. geophys., this issue.

To access this journal online:
http://www.birkhauser.ch